Composites Part B 80 (2015) 361–368

Contents lists available at ScienceDirect

Composites Part B

journal homepage: www.elsevier.com/locate/compositesb

Comparative evaluation of fiber treatments on the creep behavior of jute/green epoxy composites

Jiří Militký*, Abdul Jabbar

Department of Material Engineering, Technical University of Liberec, Studentská 2, 461 17 Liberec, Czech Republic

ARTICLE INFO

Article history:
Received 27 March 2015
Received in revised form
15 May 2015
Accepted 12 June 2015
Available online 21 June 2015

Keywords:
Biocomposites
B. Creep
B. Interface/interphase
A. Polymer-matrix composites (PMCs)

ABSTRACT

This work presents the short term creep behavior of novel treated jute fabric reinforced green epoxy composites. Jute fabric was treated with CO_2 pulsed infrared laser, ozone, enzyme and plasma. The treated jute fibers were characterized by scanning electron microscopy (SEM). Composites were prepared by hand layup method and compression molding technique. The creep and dynamic mechanical tests were performed in three-point bending mode by dynamic mechanical analyzer (DMA). The creep strain was experiential to increase with temperature. The treated composites exhibited less creep strain than untreated one at all temperatures. The best result in terms of creep deformation is presented by laser treated composite which dominantly exhibited elastic behavior rather than viscous behavior, especially at higher temperatures. The Burgers four parameters model was used to fit the experimental creep data using R statistical computing software. A good agreement between experimental data and theoretical curves were obtained. Dynamic mechanical analysis results revealed the reduction in the tangent delta peak height of treated composites, might be due to improvement in fiber/matrix interfacial adhesion. The degree of interfacial adhesion between the jute fiber and green epoxy was also anticipated using adhesion factor obtained through DMA data and laser treated composite revealed the better interlocking of fibers and matrix at the interface.

1. Introduction

The scientists and researchers have been forced to look into alternative materials in the recent years due to serious environmental and economic concerns in order to replace traditional polymer composites made with synthetic fibers such as glass and carbon etc. [1] which resulted in increasing interest in the development of bio-composites [2,3]. Bio-composites are the composites in which plant based natural fibers such as jute, hemp, flax, kenaf and/or sisal are reinforced with either biodegradable or non-biodegradable matrices [4–6]. Plant fibers have some interesting characteristics such as cost effectiveness, renewable, available in huge quantities, low fossil-fuel energy requirements, reasonably good mechanical properties and low cost compared to synthetic fibers [7]. However, the lack of interaction of these fibers with most of the matrices is a major concern for their applications as a reinforcement for bio-composites. Weak fiber/matrix interface reduces the reinforcing efficiency of fibers due to less stress transfer from the matrix to the fiber [8]. Polymer composites used in engineering applications are often subjected to stress for a long time and at high temperatures. Creep behavior is a very important end-use property for bio-composites, because both the natural fiber reinforcement and polymer matrix exhibit time and temperature dependent properties. Thus a time and temperature dependent degradation in modulus (creep) and strength (creep rupture) may occur over time, as a consequence of the viscoelasticity of the polymer matrix [9]. Considerable studies can be found in literature on the creep behavior of bio-composites. Different mathematical modeling techniques have also been applied to analyze creep behavior of composite materials [10–12]. However, creep studies taking into account the fiber/matrix adhesion are less common [10,13,14]. The objective of this work is to report the influence of some novel treatment methods such as CO_2 pulsed infrared laser, ozone, enzyme and plasma on the creep behavior and dynamic mechanical properties of woven jute/green epoxy composites.

Jute is an abundant natural biodegradable plant fiber used as a reinforcement in bio-composites [15] and occupies the second place in terms of world production levels of cellulosic fibers [16]. To

* Corresponding author. Tel.: +420 48 535 3228.
E-mail address: jiri.militky@tul.cz (J. Militký).

http://dx.doi.org/10.1016/j.compositesb.2015.06.014
1359-8368/

the authors' best knowledge, no work has been reported yet that fulfills the above mentioned objective using treated jute woven fabric as a reinforcement and green epoxy resin as a matrix system.

2. Experimental

2.1. Materials

Jute yarn of linear density 386 tex, produced from tossa jute (*Corchorus olitorius*) fibers was used to produce a woven fabric having areal density of 600 gm^{-2} with 5-end satin weave design on a shuttle loom. Warp and weft densities of the fabric were 6.3 threads per cm and 7.9 threads per cm respectively. Jute fabric was first washed with 2 wt% non-ionic detergent solution at 70 °C for 30 min prior to treatments to remove any dirt and impurities and dried at room temperature for 48 h. Green epoxy resin CHS-Epoxy G520 and hardener TELALIT 0600 were supplied by Spolek, Czech Republic. The main characteristics of the resin system are reported in Table 1 as specified by the manufacturer.

2.2. Treatment methods

2.2.1. Enzyme treatment

Untreated jute fabric was subjected to enzyme treatment. A solution, having 1%owf Texazym DLG new, 3%owf Texzym BFE and 0.2 g/l of Texawet DAF anti-foaming agent (all supplied by INOTEX, Czech Republic) in distilled water, was prepared and jute fabric was dipped in it at 50 °C for 2 h maintaining a liquor ratio of 10:1. After the treatment, the fabric was rinsed with fresh water several times and dried at room temperature for 48 h.

2.2.2. Ozone treatment

Ozone treatment was done by putting the jute fabric for 1 h in a closed container filled with ozone gas. The container was connected to ozone generator "TRIOTECH GO 5LAB-K" (TRIOTECH s.r.o. Czech Republic) which was continuously generating ozone gas at the rate of5.0 g/h. Oxygen for the production of ozone gas was generated by "Kröber O2" (KröberMedizintechnik GmbH, Germany).

2.2.3. Laser treatment

Laser irradiation was performed on the surface of jute fabric with a commercial carbon dioxide pulse infrared (IR) laser "Marcatex 150 Flexi Easy-Laser" (Garment Finish Kay, S.L. Spain), generating laser beam with a wavelength of 10.6 μm. Parameters that determine marking intensity of laser are marking speed (bits/ms), duty cycle (%) and frequency (kHz). In this study, the marking speed was set to 200 bits/ms, the duty cycle (DC) to 50% and frequency to 5 kHz. The used laser power was 100 W. Laser beams interact with fibers by local evaporation of material, thermal decomposition or changing the surface roughness [17].

2.2.4. Plasma treatment

Jute fabric was treated for 60 s with dielectric barrier discharge (DBD) plasma with discharge power of 190 W at atmospheric pressure using a laboratory device (Universal Plasma Reactor, model FB-460, Czech Republic).

2.3. Composite manufacturing

The composite laminates were prepared by hand layup method. The resin and hardener were mixed in a ratio of 100:32 (by weight) according to manufacturer recommendations, before hand-layup. The prepared resin mixture was poured on fabric layers and spread out by a hand roller. The gentle rolling action of hand roller confirmed the wetting of jute fabrics and the excess resin was squeezed out of the panel layup by the roller. Each composite laminate comprised 3 layers of jute fabric with orientation of each layer in the same direction. The composite layup along with Teflon sheets were sandwiched between a pair of steel plates and cured at 120 °C for 1.0 h in mechanical convection oven with predetermined weight on it to maintain uniform pressure of about 50 kPa [18]. The fiber volume fraction (V_f) of all composites was in the range of 0.25–0.27.

2.4. SEM analysis of jute fibers

The surface of untreated and treated jute fibers was characterized with scanning electron microscopy (SEM). The SEM photographs of jute fibers were taken using a scanning electron microscope TS5130-Tescan SEM at 20 kV accelerated voltage. The surfaces of the jute fibers were coated with gold by means of a plasma sputtering apparatus prior to SEM investigation and were investigated at 2000× magnification to observe the surface morphological changes caused by different treatments.

2.5. Characterization of composites

Creep tests were conducted in three point bending mode within the temperature range 40–100 °C in steps of 30 °C using Q800 Dynamic Mechanical Analysis (DMA) instrument of TA instruments (New Castle DL, USA). The temperature range was selected below the glass transition temperature (obtained from the loss modulus curves) of composites (Table 3).The static stress of 2 MPa was applied at the center point of long side of the sample through the sample thickness for 30 min after equilibrating at the desired temperature and creep strain was measured as a function of time. The static stress was selected after performing a strain sweep test, where the linear viscoelastic region was defined for each of the composites ensuring that the creep tests were conducted in the linear region. The dynamic

Table 1
Resin system characteristics.

Characteristics	Resin + hardener (CHS-Epoxy G520 + TELALIT 0600)
Viscosity (Pa.s, 25 °C)	3.8
Mixing ratio (pbw)	100: 32
Minimal curing temperature (°C)	20
Minimal potlife (23 °C, hours)	6
T_g (°C)	200
Flexural strength (MPa)	115
Tensile strength (MPa)	65
Elongation (%)	4
Impact strength (kJ/m^2)	20

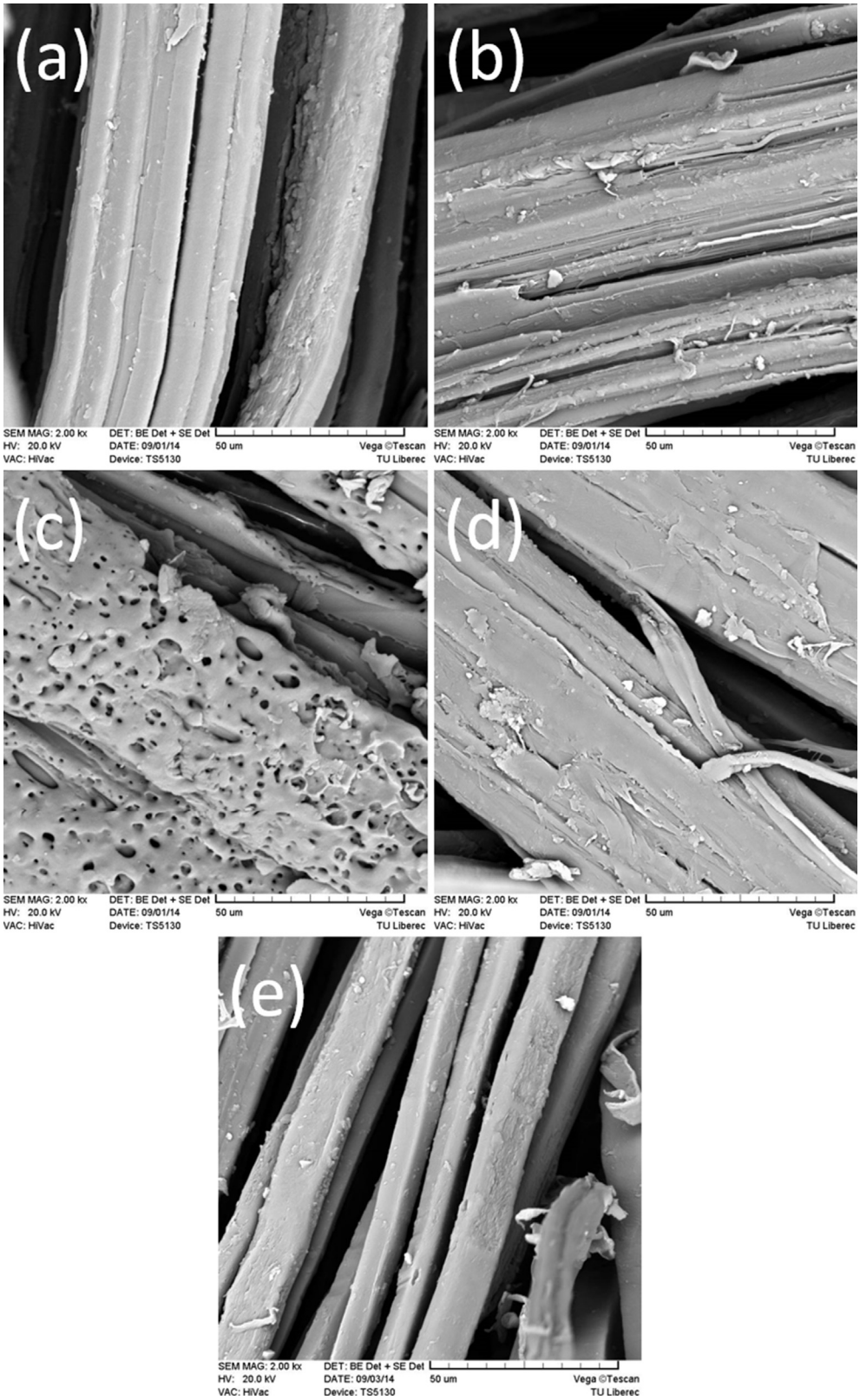

Fig. 1. Surface morphology of jute fibers: (a) untreated, (b) enzyme, (c) laser, (d) ozone, (e) plasma.

mechanical properties of composites were measured in 3-point bending mode using the above same instrument. The testing conditions were controlled in the temperature range of 35–200 °C, with a heating rate of 3 °C/min, fixed frequency of 1 Hz, preload of 0.1 N, amplitude of 20 μm, and force track of 125%. The samples having a thickness of 4.5–5 mm, width of 12 mm and span length of 50 mm were used for both creep and DMA testing. Two replicate samples were tested for each condition and average values are reported.

3. Results and discussion

3.1. Surface morphology of jute fibers

The morphological changes that occur after different treatments are examined by SEM and shown in Fig. 1. Significant changes in surface morphology are observed after treatments.

Fig. 1a shows the multicellular nature of untreated jute fiber with a rather smooth surface whereas a rough and fragmented surface morphology can be observed for enzyme treated fibers (Fig. 1b). This may be due to partial removal of cementing materials from the fiber surface after this treatment. Fig. 1c displays the thermal degradation of surface fibers after laser treatment giving a porous and rough surface of fabric. The increase in roughness and cracks are noticeable on the surface of ozone treated jute fiber (Fig. 1d). Plasma treatment causes a minor increase in fiber surface roughness. Overall; SEM micrographs give an indication that all treatments have changed the surface morphology of jute fibers.

3.2. Creep behavior

Four parameters (or the Burgers) model is one of the mostly used models to give the relationship between the morphology of the composites and their creep behavior [19,20]. It is based on a

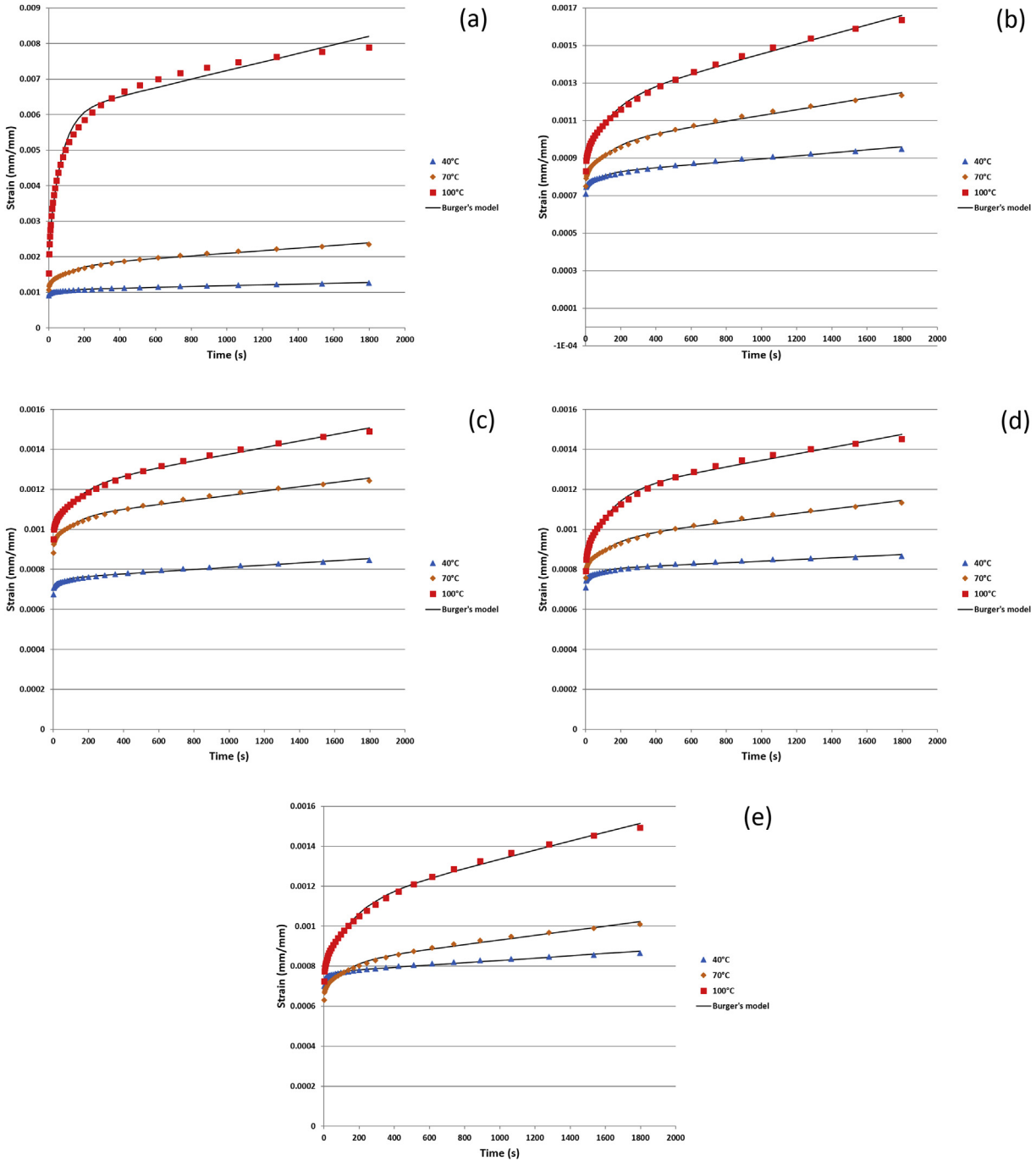

Fig. 2. Creep curves of untreated and treated jute reinforced composites: (a) untreated, (b) enzyme, (c) laser, (d) ozone, (e) plasma.

series combination of a Maxwell element with a Kelvin–Voigt element. The total creep strain is divided into three separate parts: ε_M the instantaneous elastic deformation (Maxwell spring), ε_K viscoelastic deformation (Kelvin unit) and ε_∞ viscous deformation (Maxwell dash-pot). Thus, total strain as a function of time can be represented by the following equations:

$$\varepsilon(t) = \varepsilon_M + \varepsilon_K + \varepsilon_\infty \tag{1}$$

$$\varepsilon(t) = \frac{\sigma_0}{E_M} + \frac{\sigma_0}{E_K\left(1 - e^{-E_K t/\eta_K}\right)} + \frac{\sigma_0}{\eta_M} t \tag{2}$$

where ε(t) is the creep strain, σ_0 is the stress, t is the time, E_M and E_K are the elastic moduli of Maxwell and Kelvin springs, and η_M and η_K are the viscosities of Maxwell and Kelvin dashpots. η_K/E_K is usually denoted as τ, the retardation time required to generate 63.2% deformation in the Kelvin unit [21]. ε_M is a constant value and does not change with time. ε_K represents the earliest stage of creep and attains a saturation value in short time and ε_∞ represents the trend in the creep strain at sufficiently long time, and appears similar to the deformation of a viscous liquid obeying Newton's law of viscosity.

The nonlinear regression analysis on the creep curves was performed by employing the R statistical computing software version 3.1.2. The minimum sum of squared deviation of experimental data from model values (least squares) was selected as criterion [22]. The four parameters E_M, E_K, η_M, η_K of the Burgers model were estimated by fitting the experimental data to eq. (2) and least square estimates of regression parameters were obtained by minimizing the sum of squares.

The creep behavior of jute composites with and without different fiber treatments at different temperatures (40 °C, 70 °C and 100 °C) is shown in Fig. 2. The Burgers model curves show a satisfactory agreement with the experimental data (Fig. 2). It can be observed that the composites have low instantaneous deformation ε_M and creep strain at 40 °C due to higher stiffness of composites but this deformation increases at higher temperatures due to decrease in composites stiffness. The creep strain of all composites also increased at higher temperatures but the untreated jute composite was affected more than the treated composites. When the stress is applied to the composite material, the fiber/matrix interactions are of frictional type and shear load at the interface is responsible for the matrix/interface material flow in shear [13] and untreated composite in more prone to creep due to weak fiber/matrix interface. The four parameters E_M, E_K, η_M, η_K of Burgers model, used to fit the eq. (2) to the experimental data, are summarized in Table 2. All four parameters were found to decrease for all composites as temperature increased (Table 2). E_M corresponds to the elasticity of the crystallized zones in a semicrystallized polymer. Compared to the amorphous regions, the crystallized zones are subjected to immediate stress due to their higher stiffness. The instantaneous elastic modulus is recovered immediately once the stress is removed. The decrease in parameter E_M value resulted from a decreased material stiffness (instantaneous modulus). E_K is also coupled with the stiffness of material and reduction in its value resulted from the increase in the viscoelastic deformation as temperature increased. The viscosity η_M corresponds to damage in the crystallized zones and irreversible deformation in the amorphous regions and the viscosity η_K is associated with the viscosity of the amorphous regions in the semicrystallized polymer. The decrease in parameter η_M proposes a decrease in viscosity of the bulk materials and that of η_K anticipate an improvement in the mobility of molecular chains at higher temperature. The parameters for untreated composites have undergone a largest decrease, resulting in higher creep strain (Fig. 2a). The laser and ozone treated composites have comparatively better values of parameters especially η_M which is related to the long term creep strain and validates less temperature dependence of these composites (Fig. 2c and d).

The creep strain is low for treated jute composites at all temperatures compared to untreated one as shown in Fig. 3. The less creep strain is shown by laser and ozone treated composites at all temperatures followed by plasma and enzyme treated ones. The laser treated composite has greater instantaneous elastic deformation at higher temperatures (70 °C and 100 °C) but less viscous deformation over time compared to other treated composites resulting in less creep deformation. The strain rate of untreated and laser treated jute composites and different temperatures are also shown in Fig. 4 for comparison. A large difference in strain rate of untreated and laser treated composites is clearly noticeable especially at higher temperatures. The better fiber/matrix adhesion contributes to elastic rather than viscous behavior of composite materials. The better performance of laser treated composite may be attributed to possibility of increase in mechanical interlocking

Table 2
Summary of four parameters in Burgers model for short term creep of the composites.

Temperature	Parameters	Treatments				
		Untreated	Enzyme	Laser	Ozone	Plasma
40 °C	E_m (MPa)	2095.9 ± 69.4	2685.9 ± 81.1	2846.8 ± 88.5	2697.7 ± 76.9	2761.4 ± 86.4
	E_k (MPa)	17761.7 ± 7160.8	27557.5 ± 13056.1	38654.8 ± 19501.0	34269.9 ± 16812.2	43244.2 ± 23485.5
	η_m (Pa.s)	1.67E13 ± 5.94E6	2.53E13 ± 1.04E7	3.57E13 ± 1.45E7	4.79E13 ± 3.05E7	3.44E13 ± 1.18E7
	η_k (Pa.s)	1.32E6 ± 1.37E6	2.28E12 ± 2.66E6	1.88E12 ± 2.71E6	2.28E12 ± 2.98E6	1.59E12 ± 2.52E6
	SS*	4.22E-9	2.28E-9	1.53E-9	1.76E-9	1.35E-9
	Adj. R^2	0.9822	0.97795	0.96798	0.95771	0.9692
70 °C	E_m (MPa)	1673.7 ± 115.7	2505.8 ± 90.9	2153.9 ± 62.9	2488.5 ± 79.2	2976.5 ± 109.8
	E_k (MPa)	3719.6 ± 1129.2	11303.05 ± 4056.9	15196.9 ± 5887.2	13682.5 ± 5398.7	13819.5 ± 4914.4
	η_m (Pa.s)	5.47E12 ± 2.28E6	1.31E13 ± 5.04E6	1.83E13 ± 8.05E6	1.85E13 ± 9.07E6	1.74E13 ± 7.28E6
	η_k (Pa.s)	4.36E11 ± 2.69E5	1.48E12 ± 9.97E5	1.68E12 ± 1.37E6	1.85E12 ± 1.34E6	1.71E12 ± 1.19E6
	SS*	3.71E-8	4.82E-9	3.88E-9	3.81E-9	3.43E-9
	Adj. R^2	0.98969	0.9903	0.98508	0.98696	0.98868
100 °C	E_m (MPa)	935.6 ± 262.6	2225.8 ± 103.3	1989.6 ± 63.3	2325.5 ± 113.6	2537.9 ± 124.0
	E_k (MPa)	513.9 ± 108.7	6710.2 ± 2246.4	9710.1 ± 3494.3	6157.4 ± 1826.2	6202.9 ± 1995.9
	η_m (Pa.s)	1.66E12 ± 1.05E6	7.76E12 ± 2.73E6	1.21E13 ± 4.96E6	1.24E13 ± 6.79E6	8.89E12 ± 3.64E6
	η_k (Pa.s)	3.51E10 ± 1.96E4	9.62E11 ± 5.62E5	1.35E12 ± 8.69E5	8.46E11 ± 4.53E5	9.93E11 ± 5.05E5
	SS*	1.44E-6	1.04E-8	6.04E-9	1.04E-8	9.33E-9
	Adj. R^2	0.98555	0.99268	0.9904	0.98994	0.99314

SS*: Sum of squared deviations.

between the fiber and matrix due to formation of micro-pores on fiber surface (Fig. 1c) resulting in an increase in the shear interfacial strength and lower creep deformation of the composite.

3.3. Dynamic mechanical analysis

The variation of storage modulus (E') of untreated and treated jute fiber composites as a function of temperature at frequency of 1 Hz is shown in Fig. 5a. It can be seen that there is a gradual fall in the storage modulus of all treated jute composites when the temperature is increased compared to untreated jute composite which had a very steep fall in E'. The DMA curves of the treated and untreated composites present two distinct region, a glassy region and a rubbery region [23]. The glassy region is below the glass transition temperature (T_g) while the rubbery region is above T_g. In the glassy region, components are highly immobile, close and tightly packed resulting in high storage modulus [24] but as temperature increases the components become more mobile and lose their close packing arrangement resulting in loss of stiffness and storage modulus. There is not a big difference in the storage modulus values of composites in the glassy region but all treated composites have higher values of storage modulus in the rubbery region. This might be due to better fiber/matrix interaction at the interface, decreased molecular mobility of polymer chains and better reinforcing effect of treated fibers which increases the thermal and mechanical stability of the material at higher temperatures [25] as shown prominently by laser treated jute composite (Fig. 5a).

It has been reported that T_g values obtained from loss modulus (E'') are more realistic as compared to those obtained from damping factor (tanδ) [26]. A positive shift in T_g to higher temperature for all treated jute composites is observed as given in Table 3 due to reduced mobility of matrix polymer chains and better reinforcement effect. It can be reasoned that the interfaces were markedly changed by the fiber treatments. According to Almeida et al. [27] systems containing more restrictions and a higher degree of reinforcement tend to exhibit higher T_g. The T_g increased from 105 °C for untreated to 126–146 °C for treated composites, especially the laser treated one with the value of 146 °C.

The change in damping factor (tan δ) of untreated and treated jute composites with respect to temperature is shown in Fig. 5b. Untreated composite displayed a higher tanδ peak value compared to treated composites. This may be attributed to more energy dissipation due to frictional damping at the weaker untreated fiber/matrix interface. When a composite material consisting of fibers (essentially elastic), polymer matrix (viscoelastic) and fiber/matrix interfaces is subjected to deformation, the deformation energy is dissipated mainly in the matrix and at the interface. If matrix, fiber volume fraction and fiber orientation are identical, as it is the situation in current study, then tanδ can be used to evaluate the interfacial properties between fiber and matrix. The composites

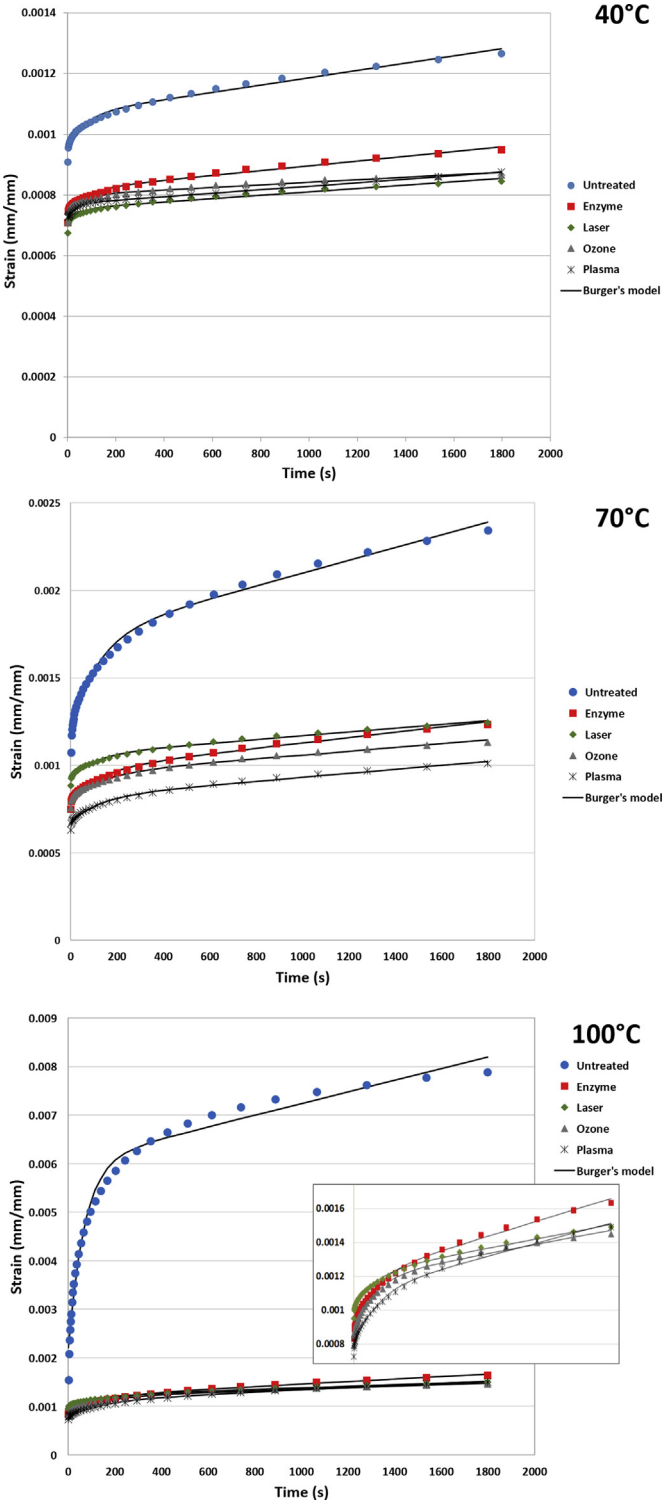

Fig. 3. Creep curves of composites at different temperatures.

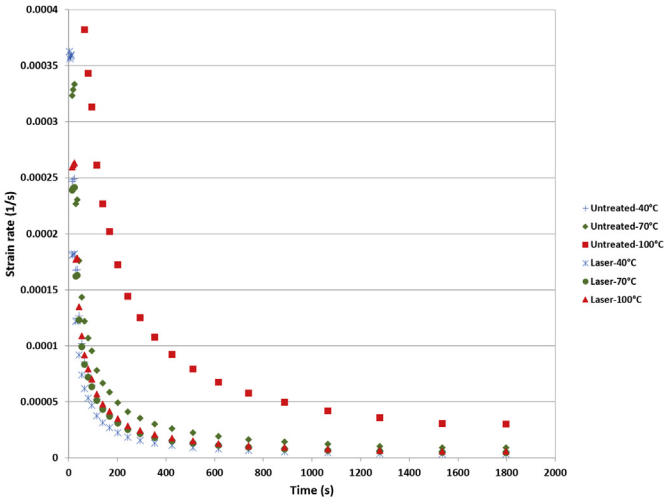

Fig. 4. Strain rate of untreated and laser treated jute composites at different temperatures.

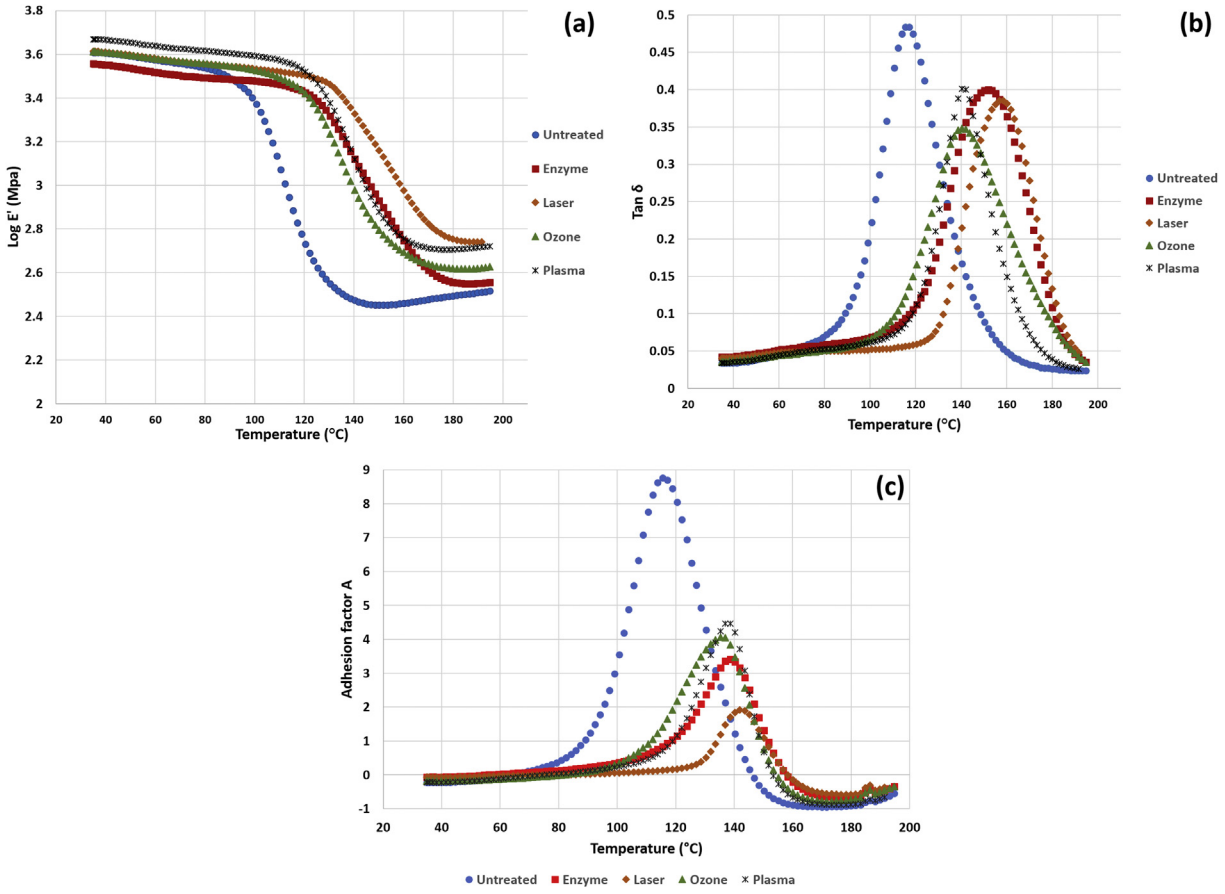

Fig. 5. Temperature dependence of (a) storage modulus, (b) tan δ and (c) adhesion factor for untreated and treated jute composites.

with poor fiber/matrix interface have a tendency to dissipate more energy than the composites with good interface bonding i.e. poor interfacial adhesion leads to greater damping [28,29]. The lower tanδ peak height is shown by ozone treated composite followed by laser treated one, among the treated composites, exhibiting a better adhesion between jute fibers and green epoxy matrix. The reduction in tanδ peak also represents the good load bearing capacity of a particular composite [30]. The broadening of tanδ peak is also observed for enzyme, ozone and laser treated samples when compared with tanδ peak of untreated composite (Fig. 5b). This indicates the occurrence of molecular relaxations at the interfacial region of composite material.

The effect of treatments on the interfacial adhesion between jute fibers and green epoxy resin was verified by adhesion factor (A) for fiber/matrix interface using the following formula;

$$A = \frac{1}{1 - Vf} \frac{\tan \delta c(T)}{\tan \delta m(T)} - 1 \tag{3}$$

where Vf is the fiber volume fraction in the composite, $\tan\delta_c\,(T)$ and $\tan\delta_m\,(T)$ are the values of tanδ at temperature T of the composite and neat matrix respectively. Low A values suggest greater interaction between the fiber and matrix. Fig. 5c expresses low adhesion factor curves of treated fiber composites compared to untreated composite which reveals the improvement in fiber matrix adhesion with fiber treatments. Laser treated composite has the lowest adhesion factor.

Table 3
T_g values obtained from E'' curve.

Composites	T_g from E''_{max} curve (°C)
Untreated	105.60
Enzymes	137.43
Laser	146.13
Ozone	126.78
Plasma	134.57

4. Conclusions

In the present work, the effect of novel treatments such as infrared laser, ozone, enzyme and plasma on the creep behavior of woven jute fabric/green epoxy composites was investigated and modeled using Burgers four parameters approach. The Burgers model fitted well the experimental creep data. The creep strain was found to increase with temperature. The treated composites showed less creep deformation than untreated one at all temperatures. The less creep deformation is shown by laser treated composite which dominantly exhibited elastic behavior rather than viscous behavior, especially at higher temperatures. This might be due to increase in fiber/matrix interaction at the interface. Dynamic mechanical tests also established that fiber/matrix interface was modified due to fiber treatments. This is also confirmed by adhesion factor curves.

Acknowledgment

This work was supported under the student grant scheme (SGS-21085) by Technical University of Liberec, Czech Republic. The author is thankful to Dr. Yasir Nawab for assistance in the

preparation of jute fabrics and Antonín Potěšil and Petr Hornik for providing DMA testing facilities.

References

[1] La Mantia F, Morreale M. Green composites: a brief review. Compos Part A Appl Sci Manuf 2011;42(6):579–88.
[2] Lu N, Oza S. A comparative study of the mechanical properties of hemp fiber with virgin and recycled high density polyethylene matrix. Compos Part B Eng 2013;45(1):1651–6.
[3] Izani N, Paridah M, Anwar U, Mohd Nor M, H'ng P. Effects of fiber treatment on morphology, tensile and thermogravimetric analysis of oil palm empty fruit bunches fibers. Compos Part B Eng 2013;45(1):1251–7.
[4] Lee B-H, Kim H-J, Yu W-R. Fabrication of long and discontinuous natural fiber reinforced polypropylene biocomposites and their mechanical properties. Fibers Polym 2009;10(1):83–90.
[5] Lu N, Oza S. Thermal stability and thermo-mechanical properties of hemp-high density polyethylene composites: effect of two different chemical modifications. Compos Part B Eng 2013;44(1):484–90.
[6] Alamri H, Low IM, Alothman Z. Mechanical, thermal and microstructural characteristics of cellulose fibre reinforced epoxy/organoclay nanocomposites. Compos Part B Eng 2012;43(7):2762–71.
[7] Mishra S, Mohanty A, Drzal L, Misra M, Parija S, Nayak S, et al. Studies on mechanical performance of biofibre/glass reinforced polyester hybrid composites. Compos Sci Technol 2003;63(10):1377–85.
[8] Hong C, Hwang I, Kim N, Park D, Hwang B, Nah C. Mechanical properties of silanized jute–polypropylene composites. J Ind Eng Chem 2008;14(1):71–6.
[9] Raghavan J, Meshii M. Creep rupture of polymer composites. Compos Sci Technol 1997;57(4):375–88.
[10] Acha BA, Reboredo MM, Marcovich NE. Creep and dynamic mechanical behavior of PP–jute composites: effect of the interfacial adhesion. Compos Part A Appl Sci Manuf 2007;38(6):1507–16.
[11] Bledzki AK, Faruk O. Creep and impact properties of wood fibre–polypropylene composites: influence of temperature and moisture content. Compos Sci Technol 2004;64(5):693–700.
[12] Marcovich NE, Villar MA. Thermal and mechanical characterization of linear low-density polyethylene/wood flour composites. J Appl Polm Sci 2003;90(10):2775–84.
[13] Hidalgo-Salazar MA, Mina JH, Herrera-Franco PJ. The effect of interfacial adhesion on the creep behaviour of LDPE–AI–Fique composite materials. Compos Part B Eng 2013;55:345–51.
[14] Xu Y, Wu Q, Lei Y, Yao F. Creep behavior of bagasse fiber reinforced polymer composites. Bioresour Technol 2010;101(9):3280–6.
[15] Corrales F, Vilaseca F, Llop M, Girones J, Mendez J, Mutje P. Chemical modification of jute fibers for the production of green-composites. J Hazard Mater 2007;144(3):730–5.
[16] Cai Y, David S, Pailthorpe M. Dyeing of jute and jute/cotton blend fabrics with 2: 1 pre-metallised dyes. Dye Pigments 2000;45(2):161–8.
[17] Štěpánková M, Wiener J, Dembický J. Impact of laser thermal stress on cotton fabric. Fibres Text East Eur 2010;18(3):80.
[18] Mishra R, Baheti V, Behera B, Militky J. Novelties of 3-D woven composites and nanocomposites. J Text Inst 2014;105(1):84–92.
[19] Ward IM, Sweeney J. Mechanical properties of solid polymers. John Wiley & Sons; 2012.
[20] Findley WN, Davis FA. Creep and relaxation of nonlinear viscoelastic materials. Courier Corporation; 2013.
[21] Yang J-L, Zhang Z, Schlarb AK, Friedrich K. On the characterization of tensile creep resistance of polyamide 66 nanocomposites. Part II: modeling and prediction of long-term performance. Polymer 2006;47(19):6745–58.
[22] Meloun M, Militky J. Statistical data analysis: a practical guide. Woodhead Publishing, Limited; 2011.
[23] Sreenivasan V, Rajini N, Alavudeen A, Arumugaprabu V. Dynamic mechanical and thermo-gravimetric analysis of *Sansevieria cylindrica*/polyester composite: effect of fiber length, fiber loading and chemical treatment. Compos Part B Eng 2015;69:76–86.
[24] Jacob M, Francis B, Thomas S, Varughese K. Dynamical mechanical analysis of sisal/oil palm hybrid fiber reinforced natural rubber composites. Polym Compos 2006;27(6):671–80.
[25] John MJ, Anandjiwala RD. Chemical modification of flax reinforced polypropylene composites. Compos Part A Appl Sci Manuf 2009;40(4):442–8.
[26] Akay M. Aspects of dynamic mechanical analysis in polymeric composites. Compos Sci Technol 1993;47(4):419–23.
[27] Almeida Jr JHS, Ornaghi Jr HL, Amico SC, Amado FDR. Study of hybrid intralaminate curaua/glass composites. Mater Des 2012;42:111–7.
[28] Pothan LA, Oommen Z, Thomas S. Dynamic mechanical analysis of banana fiber reinforced polyester composites. Compos Sci Technol 2003;63(2):283–93.
[29] Afaghi-Khatibi A, Mai Y-W. Characterisation of fibre/matrix interfacial degradation under cyclic fatigue loading using dynamic mechanical analysis. Compos Part A Appl Sci Manuf 2002;33(11):1585–92.
[30] Jawaid M, Abdul Khalil H, Hassan A, Dungani R, Hadiyane A. Effect of jute fibre loading on tensile and dynamic mechanical properties of oil palm epoxy composites. Compos Part B Eng 2013;45(1):619–24.